25th ABCM International Congress of Mechanical Engineering
October 20-25, 2019, Uberlândia, MG, Brazil

COB-2019-0837

COMPUTATIONAL STUDY OF THE NON-ISOTHERMAL TWO-DIMENSIONAL PULSED FLOW OVER A CHANNEL WITH A BACKWARD-FACING STEP

Gabriel Machado dos Santos
Ítalo Augusto Magalhães de Ávila
Hélio Ribeiro Neto
Aristeu da Silveira Neto
Federal University of Uberlândia, Av. João Naves de Ávila 2121, Campus Santa Mônica. Uberlândia, MG, Brazil, CEP: 38400-902.
gabriel.msantos@ufu.br, italo.ufuracing@gmail.com, heliorine@hotmail.com, aristeus@ufu.br

Abstract. *In the present paper, the mathematical and numerical-computational modeling of the non-isothermal pulsed flow over a backward-facing step is presented, in order to evaluate the influence of the Reynolds number and the pulse frequency over the mass and energy transport phenomena. The mathematical model is based on the classic fluid mechanics equations. For the numerical model, the finite difference method and the fractional step method for the pressure-velocity coupling are employed. Computational routines are implemented and particular cases are conducted aiming the validation of the developed computational model.*

Keywords: *computational fluid mechanics, numerical simulation, non-isothermal two-dimensional flow, pulsed flow over a backward-facing step*

1. INTRODUCTION

Analysis of flows over backward-facing steps are of great interest to numerous engineering practices. This fact is due to its high applicability in industrial processes, since the physical system, despite of its simple geometry, can be representative of several more complex processes, such as flows over spillways, flows in exhausts or refrigeration ducts and thermal energy exchangers.

The case of the flow over a step has been thoroughly studied both through computational simulations and material experiments. However, studies with pulsating flow at the entrance of the channel, as presented by Valencia and Hinojosa (1997) and Velazquez *et al.* (2008), have received less atention. This kind of problem is encountered in processes with intermittent flow, as is the case in alternative reciprocating positive displacement pumps and compressors.

This work is based on the investigation of the flow through virtual experimentation. In this manner, the physical and mathematical modeling of the problem under analysis is essential. Physical modeling consists of a representation of the real phenomenon investigated, in which physical assumptions are considered, aiming the simplification of the observed phenomenon in order to make its analysis feasible. Mathematical modeling is the determination of mathematical equations that model the physics of the problem being analised, where such equations can be algebraic, differential, integral or integral-differential.

2. PHYSICAL AND MATHEMATICS MODELING

In the present work, it is considered a channel with a discontinuity in the form of a step (Fig. 1a), where its surfaces, as well as the walls of the step, are kept at a constant temperature and assume a no-slip condition. At the channel's outlet, a Neumann boundary condition is admitted for both velocity and temperature fields. The dimensions of the channel are parameterized in relation to the step height (s): $L_{left} = 5s$, $L_{right} = 25s$ and $H = 2s$.

For the inlet, a pulsed flow condition is assumed for the horizontal velocity component (Fig. 1b). For pulse modeling, the velocity amplitude at the channel inlet is modeled as a sinusoidal function over time, as represented in Eq.. 1. For the temperature, a linear function (Eq. 2) is imposed, in order to smooth the temperature transition between the upper channel wall and the horizontal wall of the backward-facing step:

$$u_{\text{inlet}} = U_\infty \left[1 + A \sin\left(\tau St\right)\right], \tag{1}$$

$$T_{\text{inlet}} = T_{bot} + \frac{T_{top} - T_{bot}}{H - s}(y - s), \qquad \text{for} \quad y \in [s, H]. \tag{2}$$

Where A is the pulse width, St is the Strouhal number, representing the dimensionless frequency of the pulses, τ is the

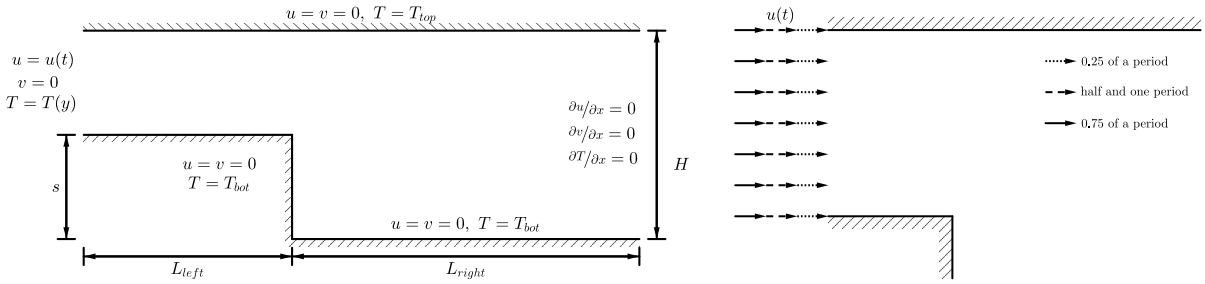

(a) Boundary conditions for the backward-facing step. (b) Inlet horizontal velocity magnitude.

Figure 1: Schematic representation of the problem addressed.

dimensionless time ($\tau = tU_\infty/H$), U_∞ is the reference velocity, y is height, measured from the channel base, T_{top} and T_{bot} are the temperatures of the upper and lower channel walls, respectively.

The equations that model the energy transport and transformations in fluid flows are obtained through the analysis of a reference element volume (REV). Therefore, it is necessary to use the Reynolds Transport Theorem (RTT), Newton's second law and the first law of thermodynamics. Initially when the mass flow balance is performed on the faces of the REV, the continuity equation is obtained in order to satisfy the mass conservation. Appllying Newton's second law to a REV, it is possible to relate the acceleration of the fluid element to the external forces acting upon it, thus obtaining the linear momentum equations. Finally, when performing the energy balance in the REV (disregarding radiation effects), one obtains the differential equation of the thermal energy.

For this study, the flow is considered to be incompressible and the fluid is modeled as Newtonian. Thus, the equations that model the movement of the fluid are given by:

$$\boldsymbol{\nabla}\cdot\mathbf{V} = 0, \tag{3}$$

$$\frac{\partial \mathbf{V}}{\partial t} + (\mathbf{V}\cdot\boldsymbol{\nabla})\,\mathbf{V} = -\frac{1}{\rho}\boldsymbol{\nabla} p - \beta(T - T_o)\mathbf{g} + \frac{\mu}{\rho}\boldsymbol{\nabla}^2\mathbf{V}, \tag{4}$$

$$\frac{\partial T}{\partial t} + (\mathbf{V}\cdot\boldsymbol{\nabla})\,T = \frac{k}{\rho c_p}\boldsymbol{\nabla}^2 T + \frac{1}{\rho c_p}\Phi, \tag{5}$$

where $\mathbf{V}$ represents the velocity vector of the fluid element, $\mathbf{g}$ the gravitational field, p is the pressure, T the local temperature, T_o the reference temperature, Φ is the viscous transformation function, ρ is the specific mass of the fluid, μ represents its dynamic viscosity, k its coefficient of thermal conductivity, c_p its thermal capacity and β is the coefficient of thermal expansion.

The characterization of the flow can be defined through some dimensionless numbers such as the Reynolds number (Re) which is related to the ratio between the inertial and viscous effects, the Prandtl number (Pr) which relates the linear momentum and thermal diffusivity, the Grashof number (Gr) which correlates the gravitational force and the force due to viscous effects, and the Nusselt number (Nu) which confronts the transfer of thermal energy by advection and diffusion.

$$Re = \frac{\rho U_\infty H}{\mu}, \tag{6}$$

$$Pr = \frac{c_p \mu}{k}, \tag{7}$$

$$Gr = \frac{g\rho^2\beta(T_{bot} - T_{top})H^3}{\mu^2}, \tag{8}$$

$$\theta = \frac{T_{bot} - T}{T_{bot} - T_{top}}, \tag{9}$$

$$Nu = \frac{H}{T_{bot} - T_{top}} \frac{\partial (T_{wall} - T)}{\partial y}\bigg|_{y=\text{wall}}, \tag{10}$$

where T_{wall} is the temperature of the wall on which the Nusselt number is evaluated and θ is the dimensionless temperature.

3. NUMERICAL-COMPUTATIONAL MODELING

Once the physical and mathematical models have been defined, one might develop a numerical-computational model. This type of modeling is employed with the purpose of obtaining approximate solutions to the equations obtained in the mathematical model. For such, the domain discretization is necessary, process in which a continuous set of information is translated into a discrete one. This way the domain is partitioned uniformly by generating the mesh $\mathcal{M}$:

$$\mathcal{M} = \{(t^n, x_i, y_j)\,;\; t^n = n\Delta t,\; x_i = i\Delta x,\; y_j = j\Delta y,\; n = 0, 1, \ldots, K,\; i = 0, 1, \ldots, L,\; j = 0, 1, \ldots, M\}\,. \tag{11}$$

where Δt is the time step, Δx and Δy are the spatial steps in the horizontal and vertical directions, respectively. The superscript n refers to temporal discretization, and similarly subindices i and j refer to spatial discretization in their respective directions.

For the solution of the equations that model the fluid dynamics (Eq. 3 and Eq. 4), the fractional step methodology is employed (Kim and Moin, 1985). In this method, for a explicit discretization, the velocity components are estimated by solving the linear momentum equations using the velocity and pressure fields at the previous time step. The pressure in the current time step is modeled as the sum of the pressure in the previous time step, plus a correction factor (Eq. 14), which is calculated using a Poisson equation (Eq. 13) obtained by combining the linear momentum and continuity equations. The current velocity field is then corrected with the pressure correction factor, so that the continuity equation is satisfied (Eq. 15). In this manner, the following system of equations is obtained:

$$\frac{\hat{\mathbf{V}} - \mathbf{V}^n}{\Delta t} = -\frac{1}{\rho}\boldsymbol{\nabla} p^n - \beta(T - T_o)\mathbf{g}^n - (\mathbf{V}^n \cdot \boldsymbol{\nabla})\,\mathbf{V}^n + \frac{\mu}{\rho}\boldsymbol{\nabla}^2\mathbf{V}^n, \tag{12}$$

$$\boldsymbol{\nabla}^2 p' = \frac{\rho}{\Delta t}\,\boldsymbol{\nabla} \cdot \hat{\mathbf{V}}, \tag{13}$$

$$p^{n+1} = p^n + p', \tag{14}$$

$$\mathbf{V}^{n+1} = \hat{\mathbf{V}} - \frac{\Delta t}{\rho}\boldsymbol{\nabla} p', \tag{15}$$

where $\hat{\mathbf{V}}$ is the estimated velocity field, p' is the pressure correction factor and the superscript n represents the time step of temporal discretization.

The system of equations mentioned above, as well as the thermal energy equation (Eq. 5), must then be discretized. For that, the finite difference method with staggered mesh is used, where the velocities are located in the faces and pressure and temperature in the center of the computational cell, as shown in Fig. 2.

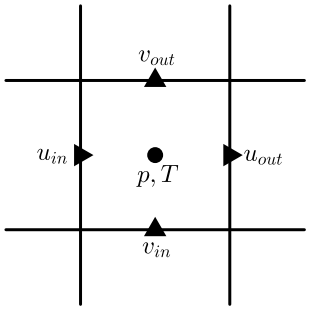

Figure 2: Representation of displaced meshes.

The Central Difference Scheme (CDS) is used for the spatial derivatives, while explicit Euler scheme is applied on the time derivative. The linear system obtained on the discrete Poisson equation is solved by the biconjugate gradient stabilized method (Van der Vorst, 1992).

The discretized equations are then implemented in computational routines using the Fortran 90 programming language. Particular cases are implemented and the computational results are compared with the literature, in order to validate the in-house developed code.

4. VALIDATION

For the validation of the developed computational model, two simulations were conducted with uniform velocity at the channel's inlet and the results are compared with the experimental results presented by Armaly *et al.* (1983). The simulations were performed under the conditions of $Re = 100$ and $Re = 389$, both with $Pr = 0.71$ and $Gr = 0$, for a uniform and regular mesh of 500×20. The results are shown in Fig. 3a and Fig. 3b, respectively.

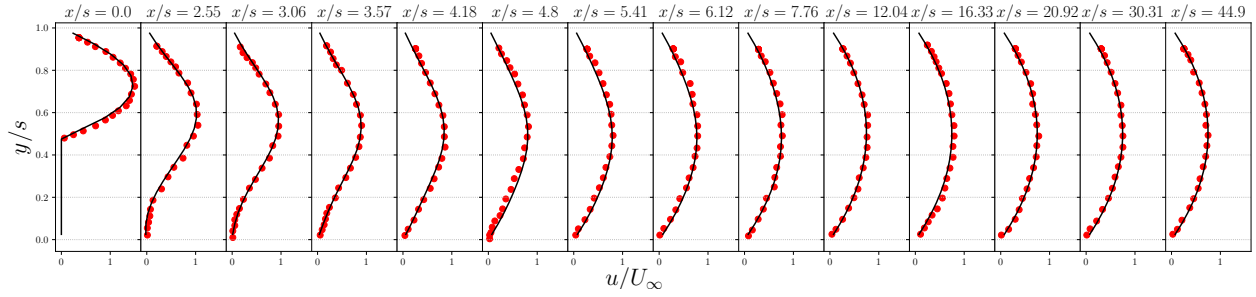

(a) $Re = 100$ and $Pr = 0.71$.

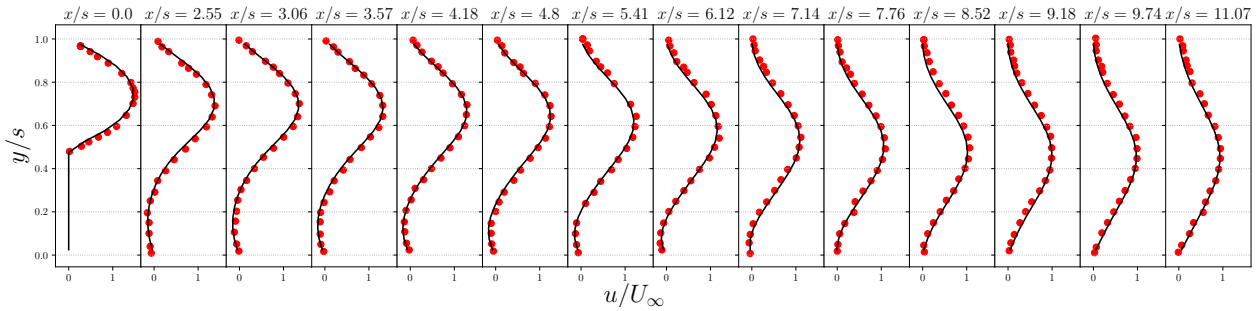

(b) $Re = 389$ and $Pr = 0.71$.

Figure 3: Profiles of the horizontal velocity component for different Reynolds values in the x/s positions: the continuous line represents the computational result obtained in the present work and points the experimental results of Armaly *et al.* (1983).

The dimensionless reattachment length downstream the backward-facing step (X_r/s) is also evaluated and compared to that measured by Armaly *et al.* (1983). For the Reynolds numbers conditions 100 and 389, the dimensionless reattachment lengths 2.69 and 8.11, respectively, are obtained. Values are close to those presented by the literature, of 2.60 and 8.20.

5. RESULTS

To analyze the influence of Reynolds number and pulse frequency on flow dynamics and energy transport, simulations were conducted for different Reynolds and Strouhal number values and the computational results obtained were analyzed. In the present work, all simulations were performed with a uniform and regular mesh of 250×20. The boundary conditions are shown in Fig. 1, where it is observed that the upper wall is kept at a constant temperature $\theta = 0$, while the step walls and the lower channel wall remain at $\theta = 1$.

The computational results presented in Fig. 4 and Fig. 5 refer to simulations performed with Reynolds numbers of 100 and 200, respectively, where we observe streamlines and temperature isocontours in different fractions of a pulse period after reaching the statistically permanent regime, where the temperature and velocity fields do not change from period to period. The dimensionless numbers that characterize the flow are kept the same for both cases and are given by $Pr = 0.71$, $Gr = 0$, $St = 1.0$ and the pulse amplitude is kept at $A = 1.0$.

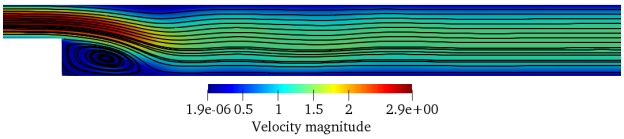

(a) Streamlines for 0.25 of a period.

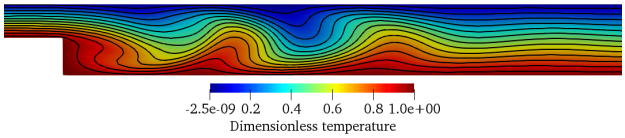

(b) Isotherms for 0.25 of a period.

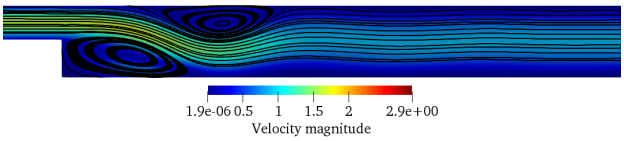

(c) Streamlines for 0.5 of a period.

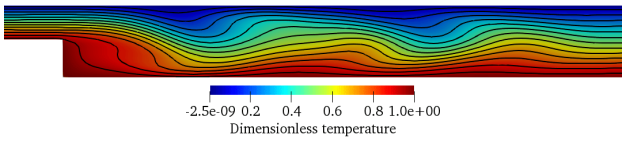

(d) Isotherms for 0.5 of a period.

Figure 4: Streamlines and isotherms in different period fractions for $Re = 100$, $Pr = 0.71$, $St = 1.0$ and $A = 1.0$.

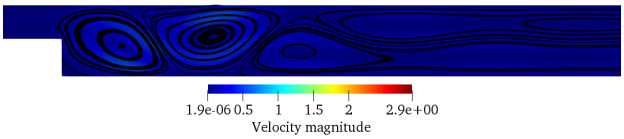

(e) Streamlines for 0.75 of a period.

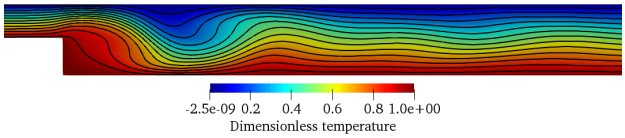

(f) Isotherms for 0.75 of a period.

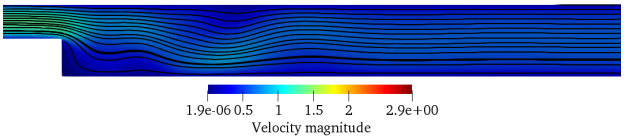

(g) Streamlines for one period.

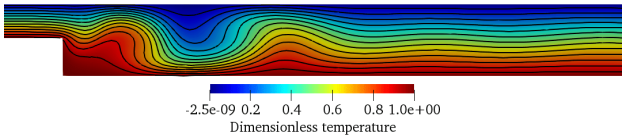

(h) Isotherms for one period.

Figure 4: Streamlines and isotherms in different period fractions for $Re = 100$, $Pr = 0.71$, $St = 1.0$ and $A = 1.0$.

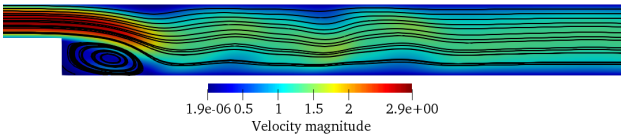

(a) Streamlines for 0.25 of a period.

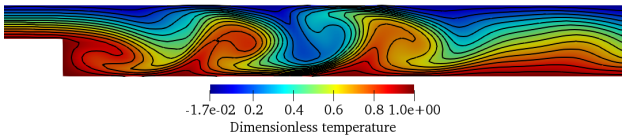

(b) Isotherms for 0.25 of a period.

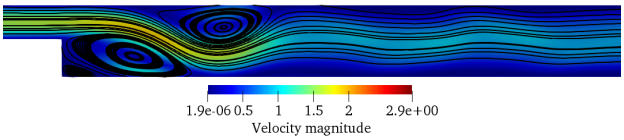

(c) Streamlines for 0.5 of a period.

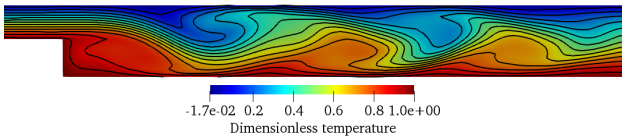

(d) Isotherms for 0.5 of a period.

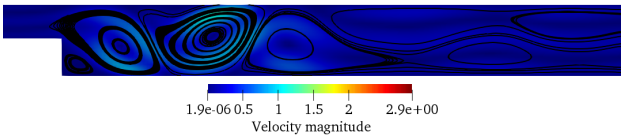

(e) Streamlines for 0.75 of a period.

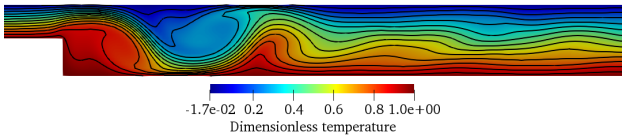

(f) Isotherms for 0.75 of a period.

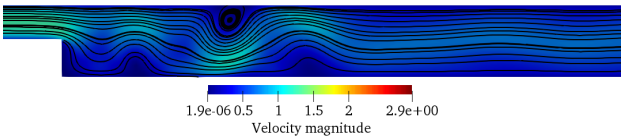

(g) Streamlines for one period.

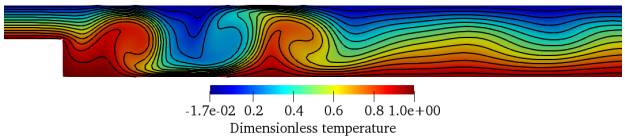

(h) Isotherms for one period.

Figure 5: Streamlines and isotherms in different period fractions for $Re = 200$, $Pr = 0.71$, $St = 1.0$ and $A = 1.0$.

The influence of the Reynolds number over the flow was analyzed by setting an unitary Strouhal number. The following Reynolds number were studied: 100, 150, and 200. The thermal boundary conditions are kept constant for each of the simulations, and the thermal characterization of the flow is given by $Pr = 0.71$ and $Gr = 0$, with pulse amplitude $A = 1.0$. The impact of the Reynolds number over the flow characteristics is analyzed by the local Nusselt number value evaluated on the upper channel wall for different period fractions of a pulse, as shown in Fig. 6.

From the analysis of Fig. 6, it is observed that the greater the Reynolds number, the greater the local Nusselt amplitudes in the upper channel wall, this happens due to the fact that higher Reynolds numbers are associated to higher velocity gradients, since an increase in the Reynolds value means that the inertial effects of flow overlaps even further the viscous effects. Thus, with higher velocity gradients, the advective thermal energy transport is favored. Since the Nusselt number is a dimensionless number that represents the ratio between the thermal energy transfer by convection and diffusion, higher local Nusselt values are expected on the channel walls.

To analyze the influence of Strouhal number on flow characteristics three Strouhal numbers were tested: 1, 2 and 3. The Reynolds number is fixed at 100. The thermal boundary conditions were kept the same, as well as the pulse amplitude at the channel inlet. The local Nusselt in the upper channel wall for different fractions of a pulse period was calculated and shown in Fig. 7.

Looking at Fig. 7 it is possible to note that the Strouhal number exerts a great influence over the frequency of the

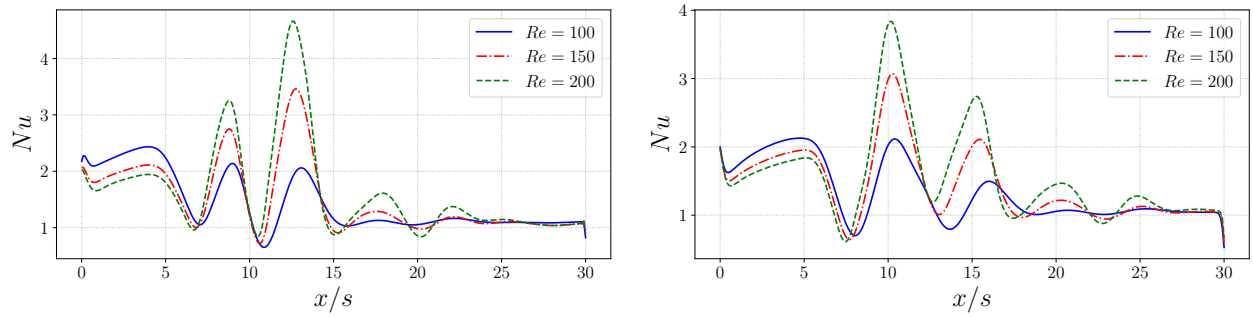

(a) 0.25 of a period.

(b) 0.50 of a period.

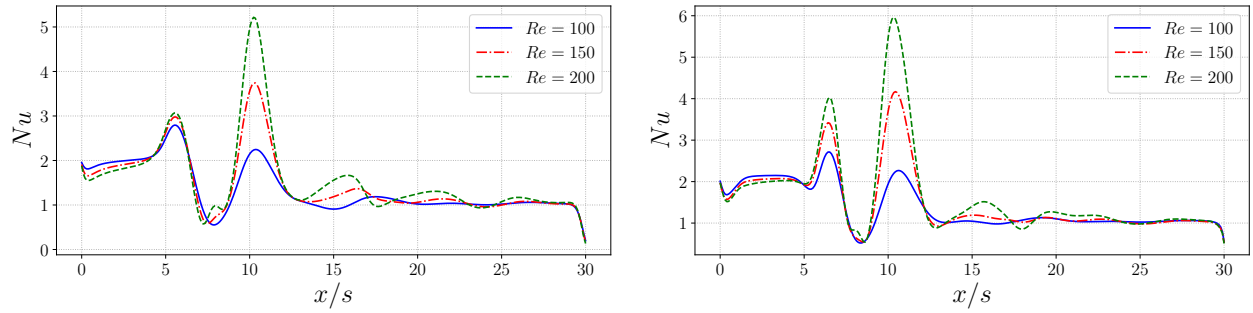

(c) 0.75 of a period.

(d) One period.

Figure 6: Local Nusselt number on the upper wall of the channel for different Reynolds number values in different fractions of pulse periods with $St = 1$, $Pr = 0.71$ and $A = 1.0$.

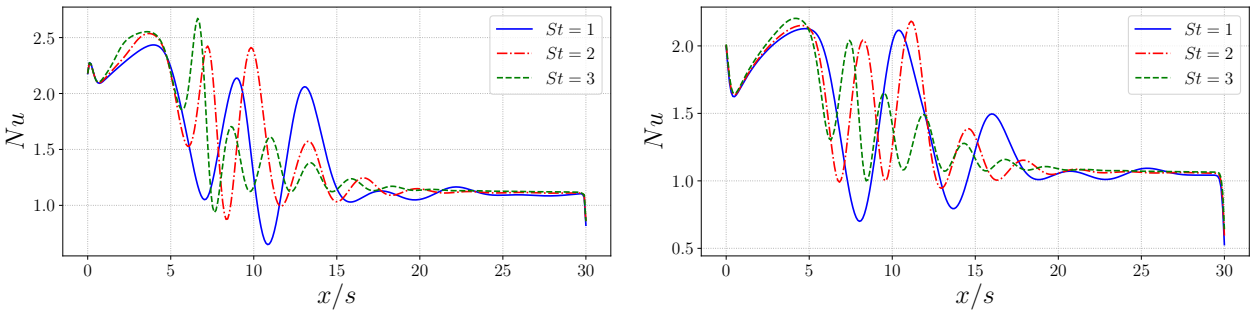

(a) 0.25 of a period.

(b) 0.50 of a period.

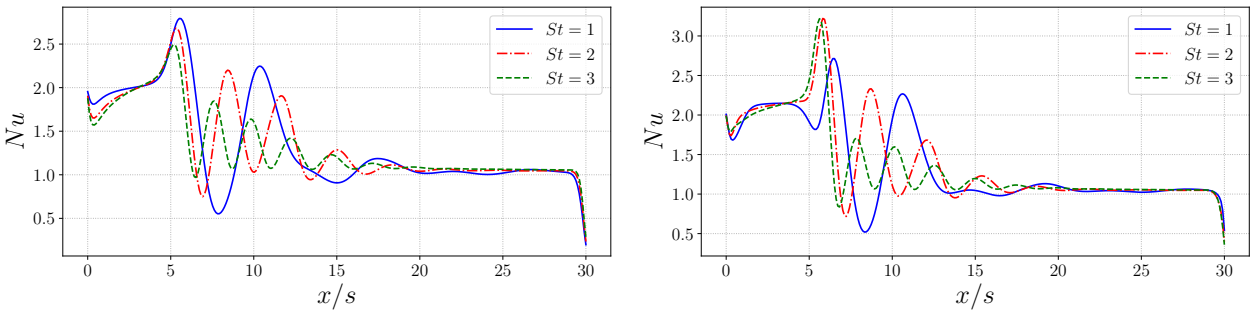

(c) 0.75 of a period.

(d) One period.

Figure 7: Local Nusselt number on the upper wall of the channel for different Strouhal number values in different fractions of pulse periods with $Re = 100$, $Pr = 0.71$ and $A = 1.0$.

local Nusselt. The Strouhal number represents the dimensionless frequency with which the pulses are generated. Thus, the larger the Strouhal, the more recirculations are formed in the channel, these recirculations transport thermal energy through the flow, directly impacting the Nusselt number.

In order to better evaluate the influence of Strouhal number on Nusselt number, two more simulations were performed

for Strouhal numbers 4 and 5, under the same conditions of the previous simulations. The results are presented on Tab. 1, where it can be observed that, in general, the average Nusselt in the upper channel wall decreases with increasing Strouhal numbers. Such phenomenon, can be explained by the fact that, increasing pulse frequencies are associated to more significant amounts of recirculations along the channel, these recirculations favor the thermal energy exchange, homogenizing the temperature along the channel, thus decreasing the gradients temperature and hence Nusselt.

Table 1: Average Nusselt number on the upper channel wall for different Strouhal values at different period fractions of a pulse with $Re = 100$, $Pr = 0.71$, and $A = 1.0$.

Strouhal \ Period fraction	$^1/_4$	$^1/_2$	$^3/_4$	1
1	1.4349	1.3376	1.3442	1.3626
2	1.4786	1.3621	1.3551	1.3972
3	1.4659	1.3416	1.3192	1.3593
4	1.4490	1.3466	1.2997	1.3114
5	1.3986	1.3849	1.2927	1.2783

The combined effect of the Reynolds number and Strouhal number on thermal energy transport is evaluated by calculating the local Nusselt number on the lower channel wall over time. Fig. 8 shows the local Nusselt calculated at a point at a distance of $5s$ downstream of the backward-facing step as a function of dimensionless time.

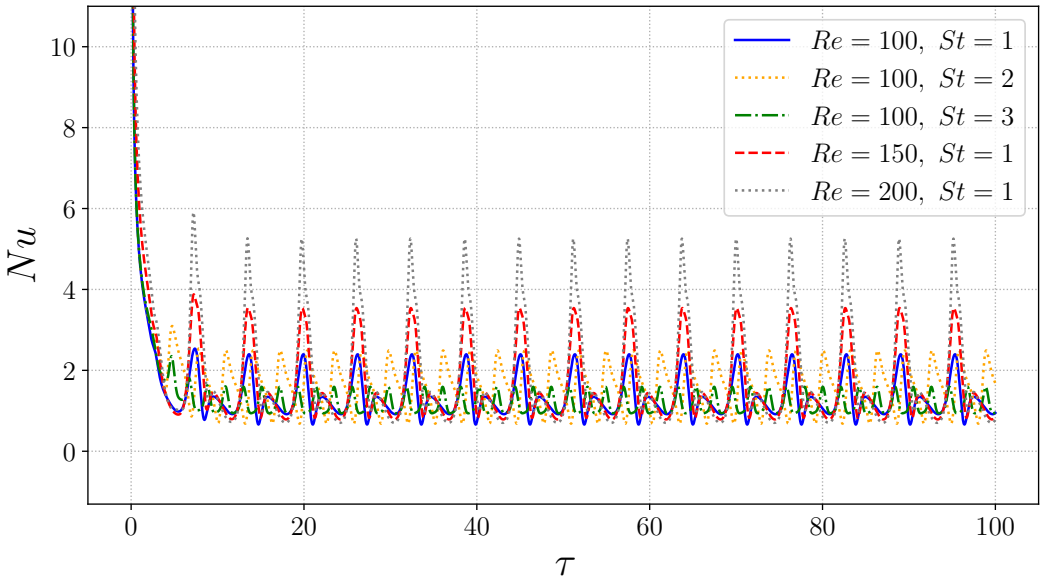

Figure 8: Local Nusselt number on the lower channel wall as a function of admensional time.

Note from Fig. 8 that the Reynolds number directly influences the Nusselt, since for larger Reynolds the Nusselt amplitudes also increase. The Strouhal number is associated with the frequency with which the Nusselt amplitudes occur and also with the average value of the Nusselt on the wall, so that with the Strouhal increase, the greater is the frequency observed on the signal, but the signal presents lower average.

6. CONCLUSION

In the present work, the physical, mathematical and numerical-computational models for the non-isothermal two-dimensional pulsed flow over a backward-facing step were presented. Computational routines were implemented using the Fortran 90 programming language. Particular cases were simulated and the results obtained were compared with the literature in order to validate the developed computational model. The small deviations between these indicated a correct modeling of the physical phenomena.

The effects of Reynolds number and Strouhal number were analyzed. It was observed that, for higher Reynolds values the thermal energy transport capacity of the flow increases. The greater the Strouhal number, the smaller the thermal energy transport capacity of the flow, a fact illustrated by the value of the Nusselt number on the channel walls.

7. ACKNOWLEDGEMENTS

The authors would like to thank Petrobras, CAPES, FAPEMIG, CNPq, MFLab and PROPP-UFU and specially the teacher Dr. João Marcelo Vedovoto for the coorientation and support in the development of this work.

8. REFERENCES

Armaly, B.F., Durst, F. and Pereira, J.C.F., 1983. "Experimental and theoretical investigation of backward-facing step flow". *Journal of Fluid Mechanics*, Vol. 127, pp. 473–496.

Kim, J. and Moin, P., 1985. "Application of a fractional-step method to incompressible navier-stokes equations". *Journal of Computational Physics*, Vol. 59, pp. 308–323.

Valencia, A. and Hinojosa, L., 1997. "Numerical solutions of pulsating flow and heat transfer characteristics in a channel with a backward-facing step". *Heat and Mass Transfer*, Vol. 32, pp. 143–148.

Van der Vorst, H.A., 1992. "Bi-CGSTAB: A fast and smoothly converging variant of Bi-CG for the solution of nonsymmetric linear systems". *SIAM Journal on Scientific and Statistical Computing*, Vol. 13, No. 2, pp. 631–644.

Velazquez, A., Arias, J.R. and Mendez, B., 2008. "Laminar heat transfer enhancement downstream of a backward facing step by using a pulsating flow". *International Journal of Heat and Mass Transfer*, Vol. 51, pp. 2075–2089.

9. RESPONSIBILITY NOTICE

The authors are the only responsible for the printed material included in this paper.